2.N

Nuclear Physics A259 (1976) 129–156, © *North-Holland Publishing Co., Amsterdam*

THE (^{12}C, ^{8}Be) REACTION ON ^{12}C, ^{16}O, ^{24,26}Mg, ^{40,48}Ca, ^{54}Fe AND ^{58}Ni BETWEEN 50 AND 65 MeV BOMBARDING ENERGY †

E MATHIAK, K. A EBERHARD, J. G. CRAMER††, H. H ROSSNER, J STETTMEIER and A WEIDINGER

Sektion Physik, Universitat Munchen, 8046 Garching, Germany

Received 8 September 1975

(Revised 2 December 1975)

Abstract: Absolute cross sections have been measured for the (^{12}C, ^{8}Be$_{g.s}$) reaction from the target nuclei ^{12}C, ^{16}O, ^{24}Mg, ^{26}Mg, ^{40}Ca, ^{48}Ca, ^{54}Fe and ^{58}Ni at various energies between 50 and 65 MeV bombarding energy (lab) using a highly efficient detection system for ^{8}Be. The results are presented in form of particle spectra and angular distributions Except for the lightest target nuclei ^{12}C and ^{16}O, the cross sections decrease rapidly with angle and a one-step direct reaction mechanism is indicated Satisfactory agreement of the data is obtained with DWBA calculations, using the finite range computer code LOLA of DeVries which treats recoil effects exactly. The spectroscopic factors extracted for the (^{12}C, ^{8}Be) reaction are close to those obtained from (^{6}Li, d), (^{7}Li, t) and (^{16}O, ^{12}C) reactions. The selective excitation of the same final states in all of these reactions, as far as data are available, and the close agreement of the spectroscopic factors are interpreted as evidence for a rather simple α-transfer in these reactions in contrast to a more complicated transfer of four nucleons

E NUCLEAR REACTIONS ^{12}C, ^{16}O, ^{24,26}Mg, ^{40,48}Ca, ^{54}Fe, ^{58}Ni (^{12}C, ^{8}Be$_{g.s}$), E = 50–65 MeV; measured $\sigma(E, E_{^8Be}, \theta)$, deduced spectroscopic factors. Enriched targets.

1. Introduction

The exceptional stability of the α-particle and the high probability of α-decay from many nuclei have led to speculations that the nucleus might be well described in terms of α-particles or other highly correlated four-nucleon structures. More recently, the tools for investigating these hypotheses have become available with the development of experimental techniques for studying four-nucleon transfer reactions such as (^{6}Li, d), (^{7}Li, t) and (^{16}O, ^{12}C). While much new information has been gained through the study of these reactions [1–4]), there remain uncertainties [5]) concerning parentages, angular momentum mismatching effects and proper treatment of finite range effects. The lithium induced reactions, e.g., have good spectroscopic overlaps for α-transfers but suffer from angular momentum mismatch problems due to the large change in mass between the incoming and outgoing particle. The (^{16}O, ^{12}C)

† Research work of J. G. Cramer and K. A. Eberhard supported in part by US Energy Research and Development Administration.

†† Permanent address: Nuclear Physics Laboratory, University of Washington, Seattle, WA 98195, USA.

reaction, on the other hand, is much better matched for most reactions, but has a rather poor spectroscopic overlap for α-transfers

We have begun investigations of an alternative transfer reaction which combines the advantages of good angular momentum matching with good spectroscopic overlap. This is the reaction (^{12}C, ^{8}Be). The nucleus ^{8}Be is particle unstable and decays into two α-particles in about 10^{-16} sec The ^{8}Be nucleus will, at a typical energy of 30 MeV, travel about 3×10^{6} fm before it decays. Thus it is well outside the range of nuclear forces before the decay takes place, but is still very likely to be within the volume of the target The reaction particle actually detected is thus not an ^{8}Be particle but a pair of α-particles.

There might, in principle, be coherent interference effects between this process and the simultaneous production of two α-particles by competing (^{12}C, 2α) reaction processes. However, the α-particles from the $^{8}\mathrm{Be}_{g.s.}$ decay are confined to a narrow momentum phase space volume by kinematics, while the three-body process will occupy a large phase space volume and is relatively weak. This insulates (^{12}C, ^{8}Be) measurements from the problems of coherent interference from three-body background.

The experimental techniques required to study reactions producing ^{8}Be as an outgoing particle offer both experimental advantages and disadvantages. These are discussed in detail in ref. [6]), but will be summarized briefly here. The detection of two coincident α-particles at the energies appropriate to an ^{8}Be ground-state decay provides a unique signature of the reaction. It provides unambiguous particle identification and also distinguishes unambiguously between excitations of the residual nucleus and the outgoing particle Since the ^{12}C beam can be stopped in a foil which readily transmits the decay α-particles, the detector can be shielded from the beam and the high counting rates arising from elastic scattering at forward angles can be "turned off". This technique permits straightforward cross-section measurements to be made at very forward angles, down to and including 0° This is of importance because many theoretical predictions can only be tested by measurements made in this region.

On the other hand, the detection of ^{8}Be particles carries with it certain disadvantages. The detection system is necessarily more complicated The effective solid angle of the detector system is reduced to about 8 to 20 % of the solid angle of the same detector array when used to detect stable particles. The finite angular acceptance of the individual detectors gives an angular uncertainty which translates to an energy spread when coincident α-particle events are analyzed and lead to an energy resolution of about 500 keV for the present system. However, both of the latter problems could be reduced or eliminated by redesigning the system so as to employ position sensitive detectors for more precise angular definition and reduction of the dead space between detectors. This is presently under construction. On the balance, we have found that the advantages offered by ^{8}Be detection outweigh the disadvantages and that, once the detection system is at hand, the measurements are simple and straightforward.

In sect. 2 the experimental procedure, in particular the detection system for ^{8}Be is described. The experimental results are presented in sect. 3; and spectroscopic factors are extracted from DWBA calculations and are compared with those from other four-nucleon transfer reactions in sect. 4.

2. Experimental procedure and ^{8}Be detection

The expected small cross sections for the (^{12}C, ^{8}Be) reactions investigated here required a highly efficient detection system for the particle unstable ^{8}Be nucleus. In addition, an intense ^{12}C beam was developed [9]) and relatively thick targets were used.

The targets used in the experiment are listed in table 1. The required thickness of the various targets was achieved by employing the so-called swing-quartz method during evaporation. A small quartz crystal was placed beside the target frames. The change in the resonance frequency caused by the target material layer evaporated onto the surface of the quartz is directly proportional to the mass of the evaporated

TABLE 1

Targets used in the experiment

Target	^{12}C	^{16}O	^{24}Mg	^{26}Mg	^{40}Ca	^{48}Ca	^{54}Fe	^{58}Ni
Thickness (μg/cm^2)	30 to 60	80 [a])	52 and 90	116	100	125	360	178
Form	self-supporting	SiO_2	^{12}C backing	^{12}C backing	^{12}C backing	^{12}C backing	self-supporting	self-supporting

[a]) The total thickness of the SiO_2 target was 150 μg/cm^2.

material on the backing. To determine the target thickness accurately the targets were weighed independently after the experiment. In addition the thickness of each target was determined from the measured elastic ^{12}C scattering yields at $E_{^{12}C}$(lab) = 15 MeV and the calculated Rutherford cross sections. An air-lock system was used to transfer the targets to the scattering chamber. During the measurements a monitor detector was placed at $\theta_{lab} = 25°$ so that a cross-section determination could be made independent of possible target inhomogeneities.

In the following we give a short outline of the ^{8}Be detection method. For a more detailed description of our system we refer to refs. [6, 9]). The particle unstable nucleus ^{8}Be in its ground and excited states at 2.9 and 11.4 MeV decays through the emission of two α-particles. For the g.s. decay, the half-life is about 10^{-16} sec and the decay energy is 93 keV. The detection of ^{8}Be events was achieved by measuring the two α-particles in coincidence. For this purpose we have developed a highly efficient detection system, consisting of eight rectangular (8 mm × 25 mm), closely adjacent

detectors. As illustrated in fig. 1, the half-angle of the maximum decay cone of the two α-particles is given by

$$\alpha_{max} = \sin^{-1} \{B/E_{^8Be}\,(\text{lab})\}^{\frac{1}{2}}, \tag{1}$$

where B is the decay energy (here 93 keV) and $E_{^8Be}$ (lab) is the ^{8}Be energy in the lab system. For the ground-state decay and for ^{8}Be energies between 10 and 65 MeV, as investigated in this paper, the maximum cone angle varied between 6° and 2° Therefore the detectors were placed closely together with a mean separation angle of 5°. The detection of $^8Be_{g.s.}$ decays is thus confined to adjacent detectors. The maximum cone angle for the decay of excited states of ^{8}Be is much larger and those events could be detected in most of the possible 28 detector combinations. The detection efficiency

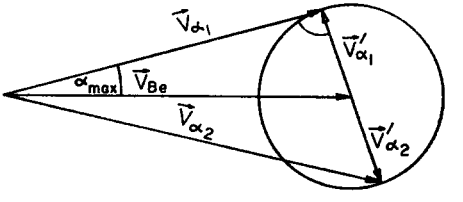

Fig 1 Velocity diagram of the ^{8}Be breakup. The resultant velocities v_{α_1} and v_{α_2} of the two breakup α-particles are calculated from the ^{8}Be velocity, $v_{^8Be}$ (before breakup), and from the two α-velocities, v'_{α_1} and v'_{α_2} due to the breakup energy (i.e 93 keV for $^8Be_{g.s.}$).

for these events, however, is substantially smaller than for $^8Be_{g.s.}$. Events from the g.s. and excited state decays can be discriminated uniquely: if ^{8}Be excited events are measured in adjacent detectors the energies of the two α-particles are very different since the decay direction of ^{8}Be is almost in the direction of the flight path of ^{8}Be. For the g.s. decay the energy difference of the two α-particles is much less because of the much lower decay energy.

Thin tantalum foils were mounted in front of each detector to prevent elastically scattered ^{12}C particles from entering the detectors This also allowed the detection of ^{8}Be events at 0°. The thickness of the tantalum foils was between 10 and 80 μm depending on the angular position of the detectors. The energies of the α-particles entering the detectors were corrected for the energy loss in the tantalum foils. Values for the energy loss were taken from ref. [7]).

The excitation energies in the resultant ^{8}Be spectra are accurate to better than $\pm$200 keV The total energy resolution is almost entirely due to kinematic broadening and therefore depends on the detector apertures and the angle at which the ^{8}Be particle is emitted. Better energy resolution could only be gained by using smaller detector apertures with the disadvantage of a reduced detection efficiency for ^{8}Be. The relatively large apertures chosen in this experiment were dictated by the small cross sections, thus leading to a relatively poor energy resolution.

The detection efficiency of the system described here has been calculated for the g s decay of ^{8}Be from the geometry of the detectors, the decay energy and the kinetic energy of ^{8}Be in ref. [8]). Typically the effective solid angles are between 0.3 and 0.8 msr. The accuracy of the efficiency calculation depends, among other quantities, critically on the precise measurement of the detector apertures. To accomplish this we have used a light source at the position of the target together with photographic paper in front of the detectors. The ^{8}Be efficiency is determined to be accurate to better than 10 %

3 Experimental results

Absolute cross sections have been measured for the four-nucleon transfer reaction (^{12}C, ^{8}Be$_{g\,s}$) from the target nuclei ^{12}C, ^{16}O, ^{24}Mg, ^{26}Mg, ^{40}Ca, ^{48}Ca, ^{54}Fe and ^{58}Ni The results are presented in form of particle spectra and angular distributions. The particle spectra serve as the basis for a discussion of the selective excitation of final states in the corresponding residual nuclei. For most states excited in the reactions angular distributions could be obtained. In sect. 4, the angular distributions are compared with distorted wave Born approximation (DWBA) calculations and spectroscopic factors are extracted.

For the presentation and discussion of the results of the various reactions we find it useful to divide the results in three groups: (i) light target nuclei [^{12}C and ^{16}O]; (ii) target nuclei strongly deformed in the middle of the sd shell [^{24}Mg and ^{26}Mg]; and (iii) target nuclei of the fp shell [^{40}Ca, ^{48}Ca, ^{54}Fe and ^{58}Ni] A reason for the separation in these groups is the fact that for light target nuclei strong compound processes are known to contribute significantly in the (^{12}C, ^{8}Be) reaction [9, 10]). A certain difference between the results in groups (ii) and (iii) can be expected from the fact that in the Mg region the nuclei are strongly deformed whereas the nuclei in group (iii) are more spherical.

For our investigations in the fp shell we have selected a group of targets for which comparable studies of the (^{16}O, ^{12}C) and/or (^{6}Li, d) reactions are available and which provide a test of the predictions of four-nucleon correlations in the corresponding residual nuclei. Four-particle configurations such as $(1f_{\frac{7}{2}})^4$ and $(2p_{\frac{3}{2}})^4$ should be preferentially excited in "α-transfer" reactions (i.e , the direct transfer of two neutrons and two protons in a tightly coupled cluster). The configuration $(1f_{\frac{7}{2}})^4$ should be the ground state four-particle band in ^{44}Ti, and the $(2p_{\frac{3}{2}})^4$ should be the corresponding band in ^{60}Zn. It is expected that extra neutrons can couple to these configurations and that neutron-neutron pair correlations can weaken the four-particle configuration. This is called the neutron blocking effect. An obvious candidate for the (^{12}C, ^{8}Be) reaction is therefore the target nucleus ^{40}Ca According to the above considerations large α-spectroscopic factors are expected for the four-particle ground-state band, since no additional neutrons are present to block these configurations (assuming no core excitation of ^{40}Ca). At ^{48}Ca, the $1f_{\frac{7}{2}}$ neutron shell is filled and so the excitation of $(1f_{\frac{7}{2}})^4$ configurations in ^{52}Ti is unlikely. However, the $(2p_{\frac{3}{2}})^4$ configuration

in ^{52}Ti could be excited. For the ^{54}Fe target the $1f_{\frac{7}{2}}$ neutron shell is filled and the $1f_{\frac{7}{2}}$ proton shell is almost filled. In this case the $(2p_{\frac{1}{2}})^4$ configuration should be more strongly excited than in case of ^{52}Ti. Finally, we decided to select a case for which the population of the $(2p_{\frac{1}{2}})^4$ configuration would be optimized. This configuration in ^{60}Zn is similar to the ground-state $(1f_{\frac{7}{2}})^4$ configuration in ^{44}Ti. Unfortunately, the obvious target for this investigation is ^{56}Ni, which is radioactive. We have therefore selected ^{58}Ni as a target. This nucleus is expected to have a dominant $\nu(2p_{\frac{1}{2}})^{-2}$ neutron configuration, with additional smaller components of $\nu(2p_{\frac{1}{2}})^{-4}(1f_{\frac{7}{2}})^2$ and $\nu(2p_{\frac{1}{2}})^{-4}(2p_{\frac{1}{2}})^2$ configurations. Thus, while this target is not ideal, it offers a relatively open $2p_{\frac{1}{2}}$ shell for the formation of four-particle configurations.

3.1. THE (^{12}C, ^{8}Be) REACTIONS ON LIGHT TARGET NUCLEI

Four-nucleon transfer reactions from light nuclei, such as ^{12}C and ^{16}O, have been studied intensively in the past few years, and numerous theoretical investigations on possible α-structures in these nuclei have been reported.

We have studied the ^{12}C(^{12}C, ^{8}Be)^{16}O reaction between incident energies of 35–69 MeV (lab). Here, we will discuss only the particle spectra and the angular distri-

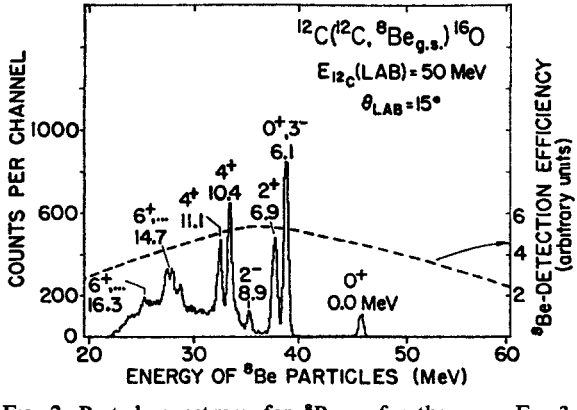

Fig. 2. Particle spectrum for ^{8}Be$_{g.s.}$ for the reaction ^{12}C(^{12}C, ^{8}Be$_{g.s.}$)^{16}O at an incident energy for $E_{^{12}C}$(lab) = 50 MeV and at θ_{lab} = 15°. The dashed curve indicates the detection efficiency as a function of the ^{8}Be energy and corresponds to the right-hand scale in the figure.

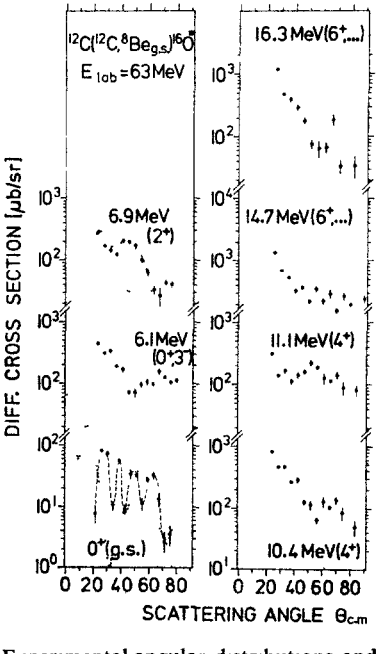

Fig. 3. Experimental angular distributions and DWBA calculations for the reaction ^{12}C(^{12}C, ^{8}Be$_{g.s.}$) ^{16}O for various final states in ^{16}O at an incident energy of $E_{^{12}C}$(lab) = 63 MeV. The DWBA calculations (dotted curve) are described in subsect. 4.1.

butions. An analysis of the excitation functions has been given elsewhere [9-11]).

3.1.1 The $^{12}C(^{12}C, ^{8}Be)^{16}O$ spectra. The most striking feature of the ^{12}C(^{12}C, ^{8}Be)^{16}O spectra is the clearly selective excitation of states in ^{16}O. Only a few states out of about forty known states in ^{16}O between excitation energies of 0 and 17 MeV are strongly populated. As an example, fig 2 shows one out of the approximately 800 spectra which were taken. The spectrum in fig. 2 corresponds to 50 MeV (lab) bombarding energy and to $\theta_{lab} = 15°$. The observed excitation energies are accurate to ± 100 keV. A detailed discussion of the ^{12}C(^{12}C, ^{8}Be)^{16}O spectra has been given in a previous paper [9])

It is interesting to note in fig. 2 that the unnatural parity state at 8.9 MeV (2^-) is relatively strongly excited A clear excitation of this state is only observed at bombarding energies of about 50 MeV or lower. The excitation of this state cannot be produced by a simple direct reaction and is interpreted in the reaction studied here as evidence for a significant compound contribution.

In the ^{12}C(^{12}C, ^{8}Be)^{16}O spectra (see fig. 2) and also in the spectra for the other (^{12}C, ^{8}Be) reactions investigated, a "background bump" is observed. Some of this background is likely to be due to random coincidences. However, since this bump does not change significantly for coincidence resolving times of 20 nsec and 100 nsec and since the energy difference of the two coincident particles was required to fulfill the condition for $^{8}Be_{g.s.}$ (see sect. 2), it is believed that most of the events in this bump actually correspond to ^{8}Be events. Independent of the target nuclei investigated the background starts at $Q = -8$ MeV and gets stronger with increasing bombarding energy. Since the binding energy of $^{8}Be + \alpha$ is about 7.2 MeV it is likely that the background bump is caused by the break-up of the projectile ^{12}C into ^{8}Be and α This is in agreement with the assumptions made by Becchetti for the (^{16}O, ^{12}C) reaction [12]).

3.1.2. The $^{12}C(^{12}C, ^{8}Be_{g.s.})^{16}O$ angular distributions. Angular distributions corresponding to various states in ^{16}O are summarized in fig. 3. For the ground state and the 6 9 MeV(2^+) state DWBA calculations, shown by the dotted lines, were performed They are described in sect. 4. The following qualitative information can be obtained from the angular distributions. whereas the angular distributions for the 4p-4h rotational band at 6.9 MeV (2^+), 10.4 MeV (4^+) and 16.3 MeV (6^+) show a strong decrease of the cross section with angle, characteristic of a one-step direct transfer process, the remaining angular distributions show a less pronounced decrease toward larger angles This difference is most clearly seen for the two 4^+ states at 10.4 and 11.1 MeV and for the (likely) 6^+ states at 14.7 and 16 3 MeV. From the fact that the 6.1 MeV angular distribution does not follow the systematics of the 4p-4h states, it is concluded that the major contribution to this angular distribution comes from the 3^- state.

In conclusion of the ^{12}C(^{12}C, ^{8}Be)^{16}O experimental results it is found that not only a direct four nucleon transfer is likely to contribute to this reaction but that also other reaction mechanisms are present. Indications are the excitation of unnatural parity states and the observation of rapid cross-section fluctuations in the excitation

functions in refs. [9-11]). These results are also confirmed by the DWBA calculations in sect. 4.

3.2. THE $^{16}O(^{12}C, ^{8}Be)^{20}Ne$ REACTION

A SiO_2 target was used to measure the $^{16}O(^{12}C, ^{8}Be)^{20}Ne$ reaction at a bombarding energy of 56 MeV. The angular range between 10° and 55° (lab) was covered in 5° steps. Similar results were obtained at 55 MeV bombarding energy and are not shown in this paper. To achieve a high detection efficiency for ^{8}Be, relatively large apertures were used in front of the detectors; this leads to an energy resolution in the spectra between 0.6 and 1 MeV (FWHM) The excitation energies in the spectra are accurate to ± 100 keV.

3.2.1. The $^{16}O(^{12}C, ^{8}Be)^{20}Ne$ spectra The spectrum in fig 4 is dominated by the selective excitation of the $K^{\pi} = 0^{+}$ [0.0 MeV (0^{+}); 1.63 MeV (2^{+}); 4.25 MeV (4^{+}); 8.75 MeV (6^{+})] and the $K^{\pi} = 0^{-}$ [5.8 MeV (1^{-}); 7.17 MeV (3^{-}); 10.3 MeV (5^{-})] rotational bands in ^{20}Ne. Both rotational bands have four-particle character: for the $K = 0^{+}$ band the four nucleons are in the sd shell, i.e., $(sd)^4$, for the $K^{\pi} = 0^{-}$ band the configuration is $(sd)^3(fp)^1$. Strong excitations of these states is also observed in other four-nucleon transfer reactions as, e.g., in (^{6}Li, d) and (^{7}Li, t)

The $[K^{\pi} = 2^{-}]$ band has a 5p-1h configuration, $(1p)^{-1}(sd)^5$ and can only be reached by removing a nucleon from the ^{16}O nucleus into the sd shell, not accessible in an α-transfer reaction The members of this band are 4.97 MeV (2^{-}), 5.63 MeV (3^{-}) and 7.0 MeV (4^{-}). The observation of states at 5.0, 5.8 and 7.2 MeV in the spectra shown in fig. 4 is a possible indication that this band is excited in the reaction. Though the energies do not agree exactly, the broadness of the states, in particular the 7.2 MeV one, seem to indicate a contribution of this band.

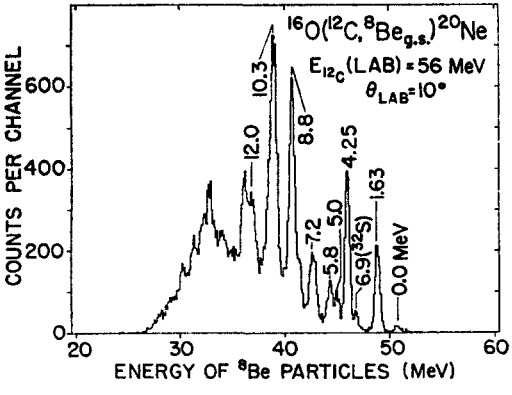

Fig. 4. Particle spectrum for the reaction $^{16}O(^{12}C, ^{8}Be_{g.s.})^{20}Ne$ measured at an incident energy of $E_{^{12}C}$(lab) = 56 MeV and at an angle of $\theta_{lab} = 10°$. The relative detection efficiency for ^{8}Be as a function of the ^{8}Be energy is shown in fig. 2

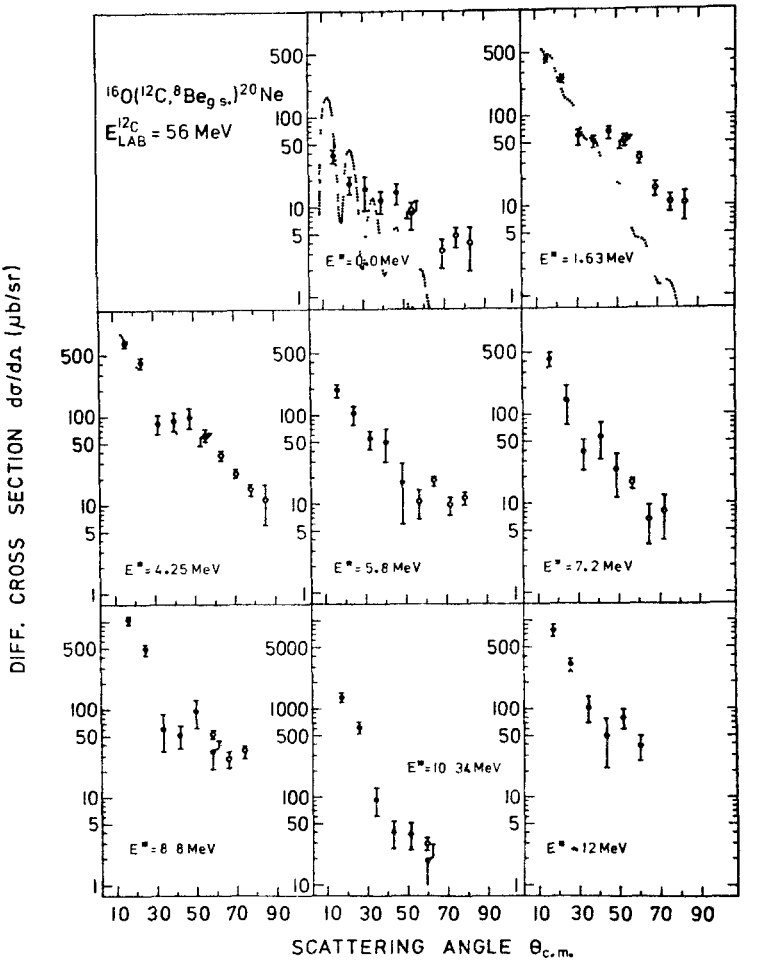

Fig 5. Experimental and calculated angular distributions for the reaction ^{16}O(^{12}C, ^{8}Be$_{g.s}$)^{20}Ne measured at an incident energy of $E_{^{12}C}$(lab) = 56 MeV for various final states in ^{20}Ne. The dotted curves are DWBA calculations and are described in subsect 4.1.

3.2.2. The $^{16}O(^{12}C, ^{8}Be)^{20}Ne$ angular distributions. Angular distributions for the observed states in the particle spectra are shown in fig. 5. An overall decrease of the cross section with angle over two orders of magnitude between angles of 20 and 90° (c.m.) is seen. This seems to indicate the overall direct character of the reaction. However, the possible excitation of unnatural parity states of the [$K = 2^-$] band with a 5p-1h configuration indicates the presence of compound nucleus or multi-step processes. A more detailed discussion on the reaction mechanism is given in sect. 4 where also the DWBA predictions are described.

3.3. THE (^{12}C, ^{8}Be$_{g.s.}$) REACTION ON sd SHELL TARGET NUCLEI

The (^{12}C, ^{8}Be) reaction has been investigated on the target nuclei ^{24}Mg and ^{26}Mg at bombarding energies of 50, 60 and 65 MeV (lab). Angular distributions were obtained between 15° and 75° (c m.). In addition, for the ^{24}Mg(^{12}C, ^{8}Be)^{28}Si reaction data were taken in 1° steps (c.m.) between −2° and 40° in order to study forward angle oscillations.

The cross sections obtained for the above reactions are of the order of 10−100 μb/sr and are significantly smaller than for the target nuclei ^{12}C and ^{16}O (see subsect 3.1). Only at 0° the cross section for the ^{24}Mg target reaches about 1mb/sr Because of the small cross sections only a limited amount of data for the ^{26}Mg target were measured. The purpose of the measurements from this target nucleus is to investigate the effect of additional neutrons as compared to ^{24}Mg

3.3.1. The ^{24}Mg(^{12}C, ^{8}Be)^{28}Si spectra. Only a few of the approximately thirty states in ^{28}Si between 0 and 10 MeV excitation energy are strongly populated in this reaction The spectrum, taken at 50 MeV (lab) bombarding energy and at 0°, is shown in fig. 6. Most strongly excited throughout the spectra are the states at 6.9 MeV and at 9.75 MeV. In fig. 6, the 9.75 MeV peak is very close to the 6.1 MeV (^{16}O) state arising from the carbon backing of the target. At other angles and energies this state is clearly separated.

Compared to the 6.9 and 9.75 MeV states the ground-state rotational band [(0.0 MeV (0$^+$); 1.78 MeV (2$^+$), 4.62 MeV (4$^+$); 8.54 MeV (6$^+$)] is only weakly excited. The weak excitation in this reaction seems to support theoretical estimates that this band has a rather complicated rotational-vibrational structure.

Above 10 MeV excitation energy the population of states in ^{28}Si near 11, 12, 13.1, 14 6 and 15.8 MeV is observed. Excitation of unnatural parity states at 6.27 MeV (3$^+$)

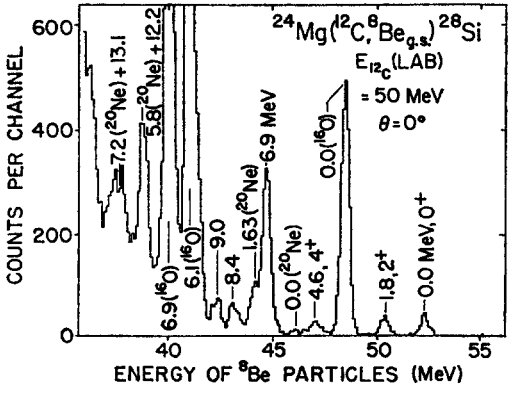

Fig. 6 Particle spectrum for the reaction ^{24}Mg(^{12}C, ^{8}Be$_{g.s.}$)^{28}Si measured at an incident energy of $E_{^{12}C}$(lab) = 50 MeV and at an angle of $\theta = 0°$. The relative detection efficiency of ^{8}Be$_{g.s.}$ as a function of the ^{8}Be energy is shown in fig. 2. Peaks corresponding to the ^{12}C backing and ^{16}O impurities are labeled in the figure.

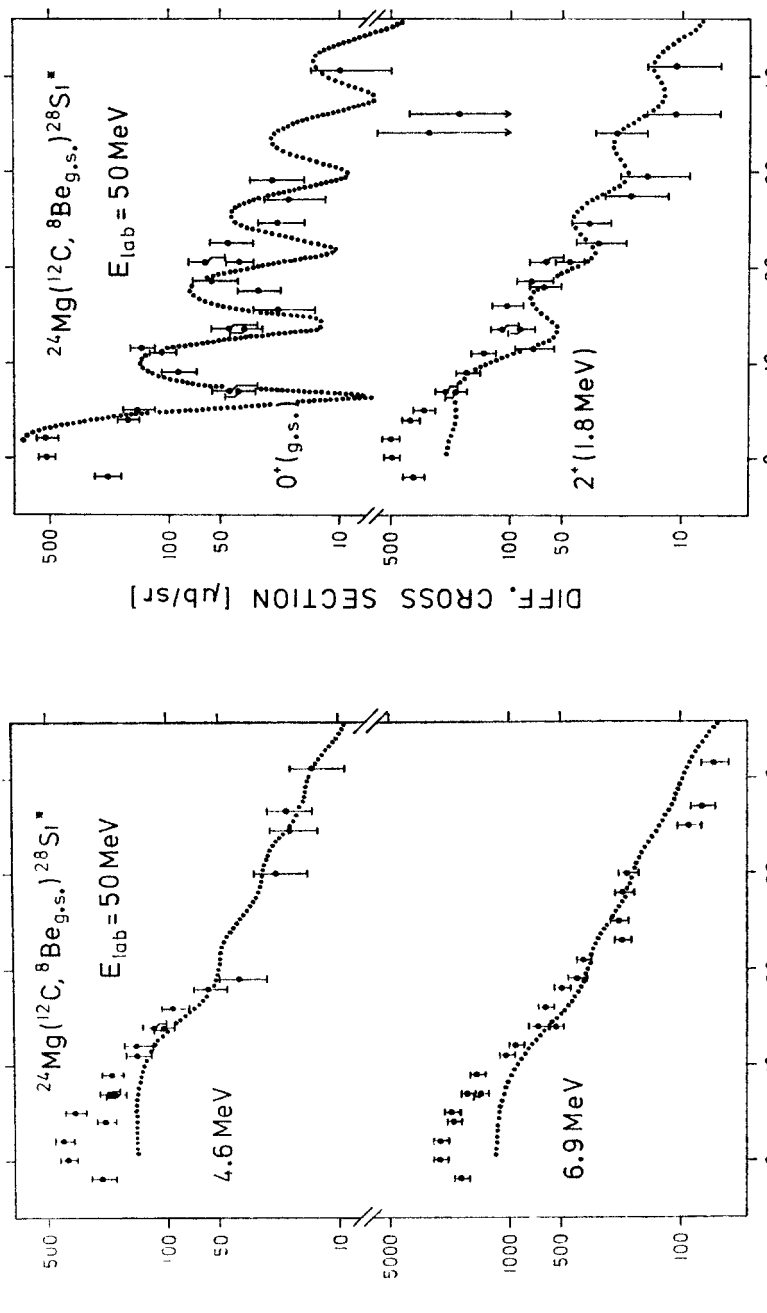

Fig 7. Angular distributions between −2° and +40° for the reaction ^{24}Mg(^{12}C, ^{8}Be$_{g.s.}$)^{28}Si to the g.s. and to excited states at 1.8, 4.6 and 6.9 MeV in ^{28}Si measured at an incident energy of $E_{^{12}C}$(lab) = 50 MeV. The dotted curves are DWBA calculations; they were calculated with the parameters given in tables 2 and 3 and they are described in subsect. 4.2.

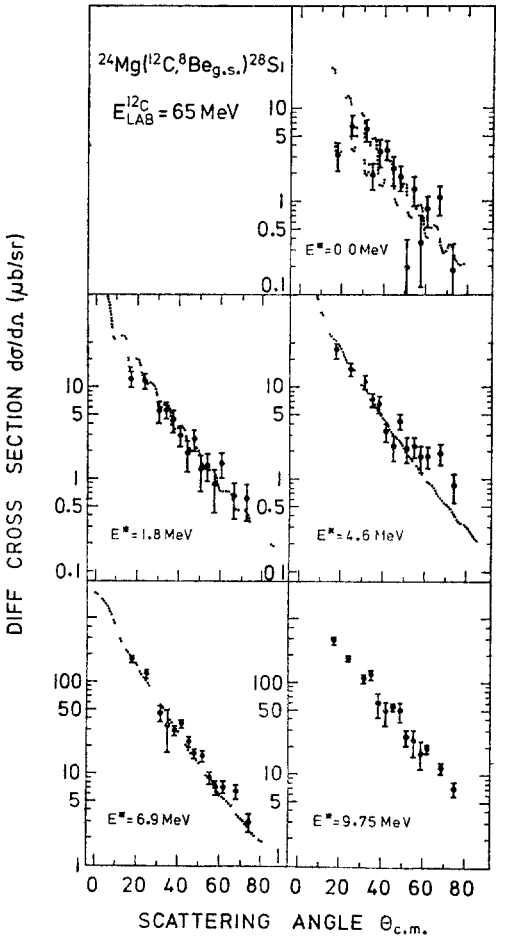

Fig. 8. Angular distributions for the ^{24}Mg(^{12}C, ^{8}Be)^{28}Si reaction at an incident energy of $E_{^{12}C}$(lab) = 65 MeV to the ground state and various excited states in ^{28}Si The dotted curves are DWBA calculations obtained with the parameters given in tables 2 and 3, these calculations are described in subsect. 4 2

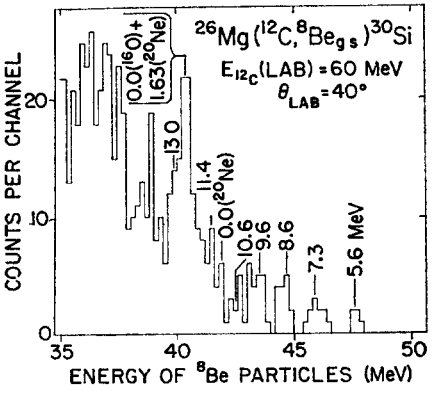

Fig 9. Particle spectrum for the ^{26}Mg(^{12}C, ^{8}Be$_{g.s.}$)^{30}Si reaction at an incident energy of $E_{^{12}C}$(lab) = 60 MeV measured at an angle of θ_{lab} = 40°. The relative detection efficiency for ^{8}Be$_{g.s.}$ as a function of the ^{8}Be energy is shown in fig 2

and 7.8 MeV (3^+) are not observed in this reaction A possible excitation of the 4^- state at 8.41 MeV could not be distinguished from the 6^+ state at 8 54 MeV

3.3.2. The ^{24}Mg(^{12}C, ^{8}Be)^{28}Si angular distributions. In figs. 7 and 8 angular distributions are shown for 50 and 65 MeV bombarding energy (lab), respectively. The error bars in figs. 7 and 8 represent the combined uncertainties from counting statistics, separation of the lines in the spectra, background subtraction and detection efficiency for ^{8}Be.

The data at 50 MeV bombarding energy (lab), measured between $-2°$ and 40° (c m) and shown in fig 7, exhibit a strongly oscillating angular distribution for the ground-state transition and exponentially decreasing angular distributions for the other states. Pronounced maxima of the cross sections are observed at 0° with cross sections of the order of 500 μb/sr for the 0^+, 2^+ and 4^+ states and an order of magnitude larger cross sections for the 6 9 MeV state For discussion of the DWBA predictions we refer to sect 4.

Angular distributions, taken in larger angular steps between 20° and 80° for a bombarding energy of 65 MeV (lab), are shown in fig. 8; the cross sections are generally smaller than at 50 MeV. Again, one observes a strong decrease of the cross section by about three orders of magnitude with increasing angle The angular distributions corresponding to the 6 9 and 9.75 MeV states show an order of magnitude larger cross section than the other states

3 3.3. The $^{26}Mg(^{12}C, ^{8}Be)^{30}Si$ spectra This reaction was chosen to investigate the (^{12}C, ^{8}Be) reaction from a "non-α-like" target nucleus and the effect of additional neutrons. In fig 9 the spectrum for the ^{26}Mg(^{12}C, ^{8}Be)^{30}Si reaction at 60 MeV bombarding energy (lab) and at 40° (lab) is shown. The energy resolution is about 600–800 keV and the excitation energies indicated in the figure are accurate to $\pm$200 keV.

The overall feature of the spectrum in fig 9 is the lack of any strongly excited states except those due to contaminants. In none of the spectra obtained states were excited with a cross section larger than 10 μb/sr. No states below 5.6 MeV are excited. In particular, the ground state ($K = 0^+$) rotational band, predicted from the SU(3) model, at 0 0 MeV (0^+) 2 23 MeV (2^+) and 5 28 MeV (4^+) is not observed in the spectra taken for this reaction

The line at 5.6 MeV probably contains contributions from the 5 37 MeV (0^+), 5 49 MeV (3^-) and 5.61 MeV (2^+) states. At 7.3 MeV several states are also likely to contribute. they are the 7 27 MeV (2^+), 7 22 MeV (4^+) and 7.43 MeV (0^+) states. Unnatural parity states at 7.1 MeV (1^+, 2^-, 3^+) and at 7.5 MeV (0^-, 2^-) probably do not contribute to this state since other unnatural parity states at 2.79 MeV (1^+) and at 4 83 MeV (3^+) are not excited in the reaction.

Above 8 MeV lines are observed in the spectrum at 8.6, 9.6, 10.6, 11 4 and 13.0 MeV Some of these states possibly could have α-structures with ^{32}S-2h configuration.

3 3 4 The $^{26}Mg(^{12}C, ^{8}Be)^{30}Si$ angular distributions. Angular distributions obtained at a bombarding energy of 60 MeV (lab) for states corresponding to excitation energies of 5 6, 7.3, 8.4–8 8, and 9.6 are shown in fig. 10. The relative large error bars are mainly due to poor counting statistics and due to uncertainties in peak integration. The cross sections are of the same order of magnitude as for the g s. rotational band in the ^{24}Mg(^{12}C, ^{8}Be)^{28}Si reaction

In summary, it can be concluded from the experimental results obtained for the sd shell nuclei that (i) the selective excitation of states in the residual nucleus ^{28}Si, (ii) the absence of unnatural parity states in the spectra and (iii) the rapid decrease of the cross section with angle are clear indications of a direct, one-step reaction process.

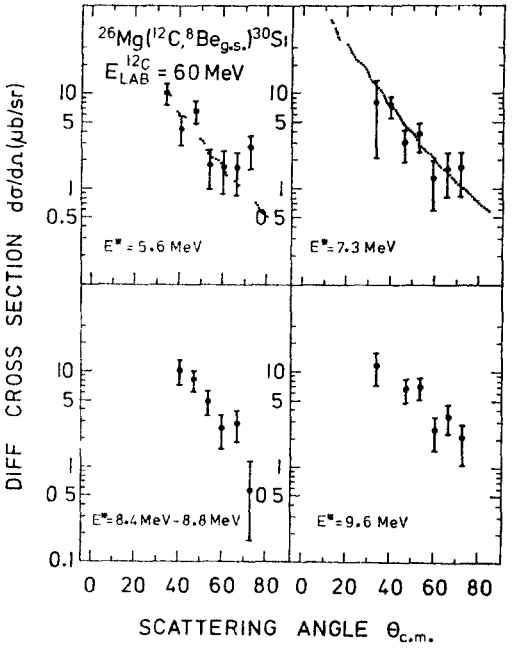

Fig. 10. Cross sections for the ^{26}Mg(^{12}C, ^{8}Be$_{g.s.}$)^{30}Si reaction at a few forward angles measured at $E_{^{12}C}$(lab) = 60 MeV for excited states in ^{30}Si around 5.6 MeV, 7.3 MeV, between 8.4 and 8.8 MeV, and around 9.6 MeV. The dotted curves are DWBA calculations obtained with the parameters listed in tables 2 and 3; these calculations are described in subsect. 4 2.

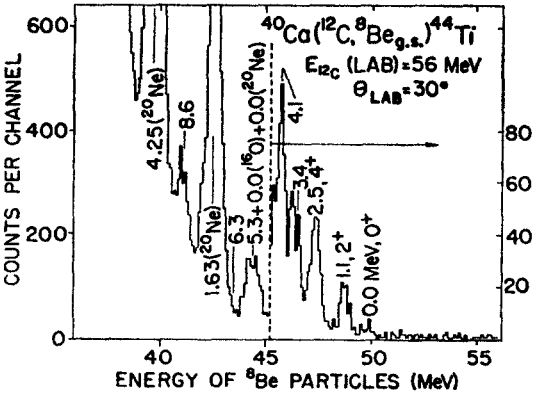

Fig. 11. Particle spectrum for the ^{40}Ca(^{12}C, ^{8}Be$_{g.s.}$)^{44}Ti reaction measured at an incident energy of $E_{^{12}C}$(lab) = 56 MeV and at a lab angle of approximately 30°. The high energy part of the spectrum is enlarged by a factor of five to show more details. The corresponding scale is on the right hand side of the figure. The relative detection efficiency for ^{8}Be as a function of the ^{8}Be energy is shown in fig. 2

The question of an actual α-transfer mechanism is discussed in sect. 4 on the basis of the DWBA calculations.

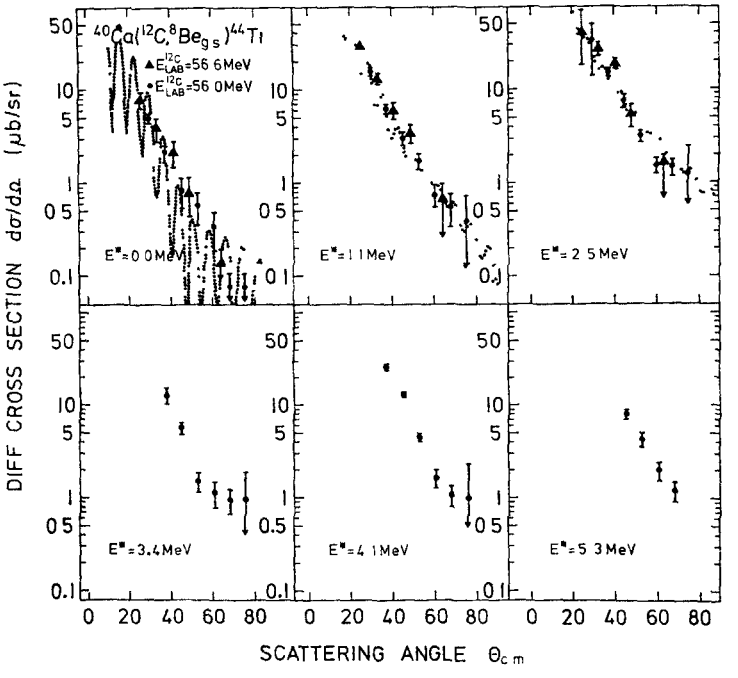

Fig. 12 Experimental and calculated angular distributions for the reaction ^{40}Ca(^{12}C, ^{8}Be$_{g.s}$)^{44}Ti to various states in the residual nucleus ^{44}Ti. The experimental cross sections were mesured at an incident energy of $E_{^{12}C}$(lab) = 56 and 56.6 MeV as indicated in the figure. The dotted curves are DWBA calculations obtained with the parameters listed in tables 2 and 3; these calculations are described in subsect 4.3.

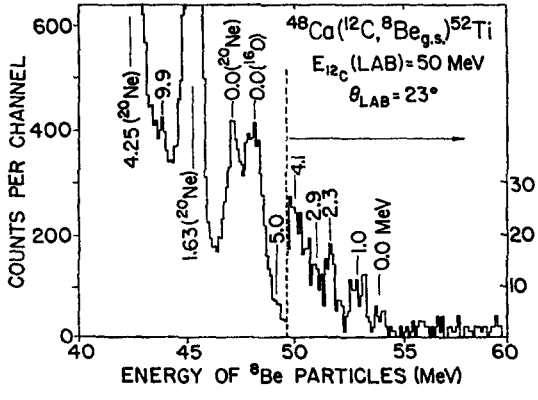

Fig 13. Particle spectrum for the ^{48}Ca(^{12}C, ^{8}Be$_{g.s}$)^{52}Ti reaction measured at an incident energy of $E_{^{12}C}$(lab) = 56 MeV and at a lab angle of approximately 23°. The high energy part of the spectrum is enlarged by a factor of ten to show more details. The corresponding scale is on the right hand side of the figure. The relative detection efficiency of ^{8}Be as a function of the ^{8}Be energy is shown in fig 2

3.4. THE (^{12}C, ^{8}Be) REACTION ON fp SHELL TARGET NUCLEI

Spectroscopic considerations and available data from other four-nucleon transfer reactions have led us to investigate the (^{12}C, ^{8}Be) reaction from the target nuclei ^{40}Ca, ^{48}Ca, ^{54}Fe, and ^{58}Ni. The small cross sections (generally between 0.1 and 10 μb/sr) along with the fact that the detection efficiency for ^{8}Be is only a few percent make these investigations difficult. Relatively large detector apertures were chosen to maximize the detection efficiency. The energy resolution obtained for the ^{8}Be spectra is between 500 keV and 1.5 MeV, depending on the ^{8}Be energy and the angle at which the particular spectra were taken. The excitation energies are accurate to $\pm$150 keV.

In the following the experimental results are presented. Spectroscopic factors, derived from DWBA calculations, are given and compared with other reactions in sect. 4.

3.4.1. The $^{40}Ca(^{12}C, ^{8}Be)^{44}Ti$ spectra and angular distributions. This reaction was investigated at 56 and 56.6 MeV bombarding energy (lab). Fig. 11 shows the spectra taken at 56 MeV bombarding energy (lab) and at 29.75° (lab). One can see the excitation of the ground state (0^+) and of states at 1.1 MeV (2^+), 2.5 MeV (4^+), 3.4 MeV and 4.1 MeV. Above 5 MeV excitation energy the spectrum is contaminated from contributions from the target-backing ^{12}C and from ^{16}O contributions. At larger angles and/or where the spectra are free of contaminations strongly excited states are observed at 5.3 MeV, between 6.8 and 7.8 MeV, and at 8.6, 10.4, 11.6 and 12.4 MeV.

Because of the contaminations in the spectra, complete angular distributions in the angular range 20°–80° (c.m.) could only be obtained for the states at 0.0, 1.1, 2.5, 3.4, 4.1 and 5.3 MeV; they are shown in fig. 12. Since no strong energy dependence of the cross section is expected, the data for the 56.0 and 56.6 MeV measurements are included in the same graph, as indicated in the figure. The overall behavior of the angular distributions is similar to those of the sd shell nuclei, though the decrease of the cross section with angle is more rapid here. At angles of about 20° the cross sections are of the same order of magnitude for comparable states in the sd shell region.

3.4.2. The $^{48}Ca(^{12}C, ^{8}Be)^{52}Ti$ spectra and angular distributions. This reaction was measured between 15° and 75° (c.m.) at a bombarding energy of 56 MeV. The low-lying states in ^{52}Ti (see fig. 13) are only weakly excited, and the cross sections (see fig. 14) are about a factor of five smaller than for the ^{40}Ca reaction. Inspection of the particle spectra obtained shows that the selectivity is less pronounced here than in ^{44}Ti which is likely to be due to the additional eight neutrons.

No separated states above 4 MeV are observed within the experimental energy resolution. Thus the question whether $(2p_{\frac{1}{2}})^4$ configurations are excited cannot be answered on the basis of the data presented here.

3.4.3. The *$^{54}Fe(^{12}C, ^{8}Be)^{58}Ni$ spectra and angular distributions* Cross sections for this reaction were measured at 56 MeV bombarding energy (lab) at angles between 10° and 40° (c.m.). A spectrum taken at 15° (lab) is shown in fig. 15. Above 20° most strongly excited is the state at 4.6 MeV. The ground-state band [0.0 MeV (0^+);

1.45 MeV (2^+); 2.45 MeV (4^+)] is clearly seen in fig. 15. The cross sections (see fig. 16) are not larger than those for the ground-state band in ^{52}Ti, as expected (see beginning of this section). Above 5 MeV, excitations are found at 6.8, 7 7 and 8 9 MeV.

The somewhat better resolution in this spectrum than in the previous ones results from a reduced kinematic broadening due to the heavier target nucleus and due to the fact that this spectrum was taken at a more forward angle.

3.4.4. The $^{58}Ni(^{12}C, ^{8}Be)^{62}Zn$ spectra and angular distribution. Data for this reaction were obtained only at angles of θ_{lab} = 30°, 35°, 40° and 45° and at a bombarding energy of 55 MeV (lab). In fig. 17 the spectrum obtained at 40° is shown The energy resolution in this spectrum is about 500 keV. Strongly excited states at 3.2, 4.0 and 5.0 MeV and a particularly strong state at 7.0 MeV are observed. The 3.2 MeV state could correspond to the 3.22 MeV (3^-) state according to Kusakari *et al.* [13]) or to the 4^+ state at 3.216 MeV given by Farwell *et al.* [14]).

The ground-state band [0.0 MeV (0^+); 0.95 MeV (2^+); 2.2 MeV (4^+)] is only weakly excited compared to states above 3 MeV. However, they are significantly

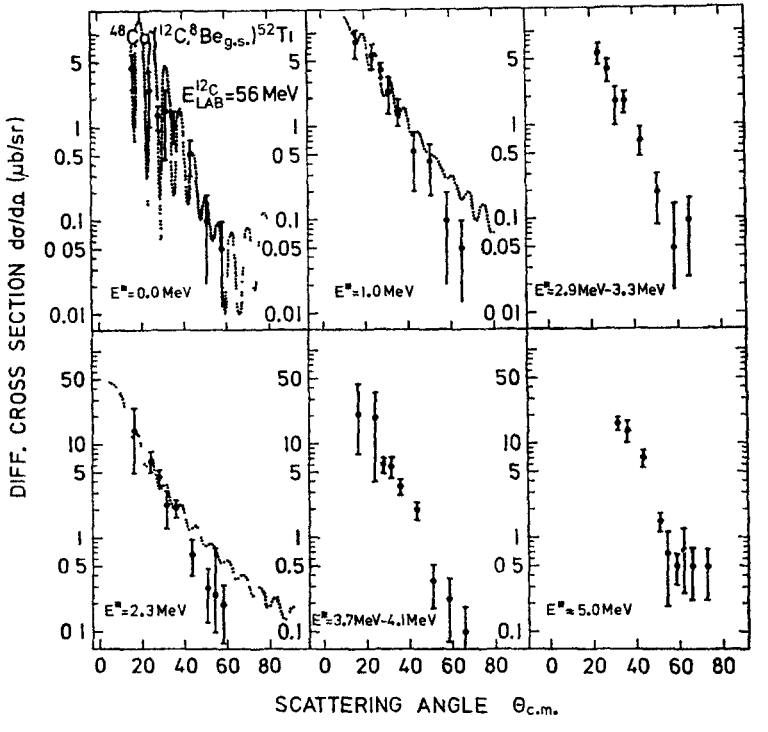

Fig 14. Experimental and calculated angular distributions for the ^{48}Ca(^{12}C, ^{8}Be$_{g.s.}$)^{52}Ti reaction measured at an incident energy of $E_{^{12}C}$(lab) = 56 MeV. The dotted curves are DWBA calculations obtained with the parameter values listed in tables 2 and 3; these calculations are described in subsect 4.3.

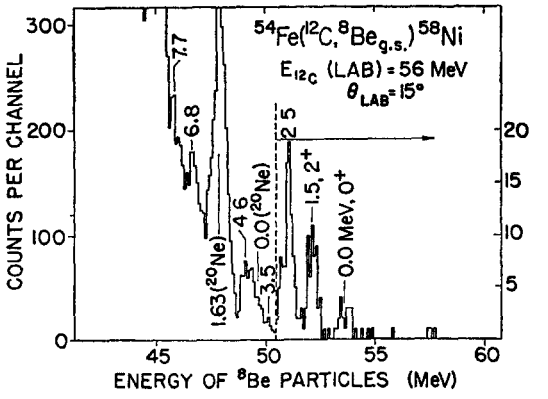

Fig. 15. Particle spectrum for the reaction ^{54}Fe(^{12}C, ^{8}Be$_{g.s.}$)^{58}Ni measured at an incident energy of $E_{^{12}C}$(lab) = 56 MeV and at a lab angle of 15°. The higher energy part of the spectrum is enlarged by a factor of ten to show more details. The corresponding scale is on the right hand side of the figure

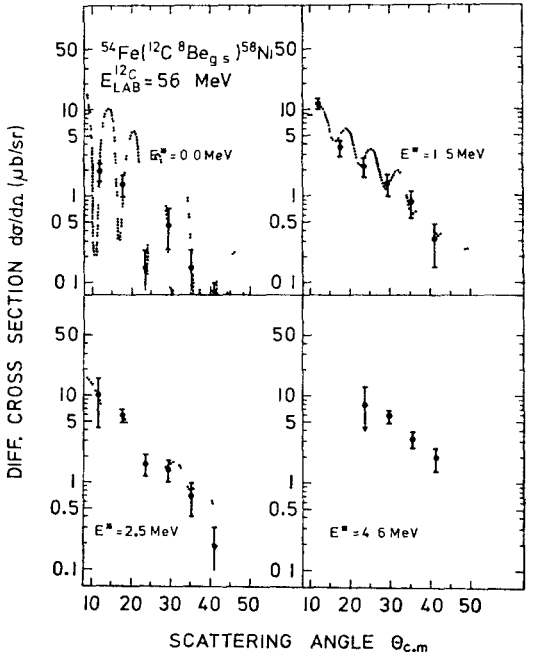

Fig. 16. Experimental cross sections for the ^{54}Fe(^{12}C, ^{8}Be$_{g.s.}$)^{58}Ni reaction measured at an incident energy of $E_{^{12}C}$(lab) = 56 MeV at a few angles between 10° and 50°. The dotted curves are DWBA calculations obtained with parameter values listed in tables 2 and 3. These calculations are described in subsect. 4.3

stronger excited than the corresponding states in ^{58}Ni and ^{52}Ti, compared with the states in ^{44}Ti the excitation is weaker here.

As shown in fig. 18, the cross sections show a similar decrease with angle as observed for the other fp shell nuclei.

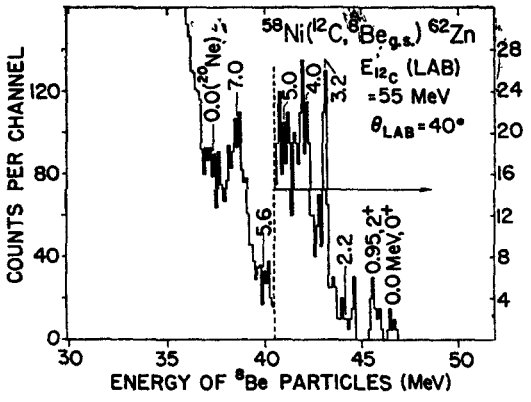

Fig. 17. Particle spectrum for the ^{58}Ni(^{12}C, ^{8}Be$_{g.s.}$)^{62}Zn reaction measured at an incident energy of $E_{^{12}C}$(lab) = 55 MeV and at a lab angle of 40°. The high energy part of the spectrum is enlarged by a factor of five to show more details. The corresponding scale is on the right hand side of the figure. The relative detection efficiency of ^{8}Be as a function of the ^{8}Be energy is shown in fig. 2

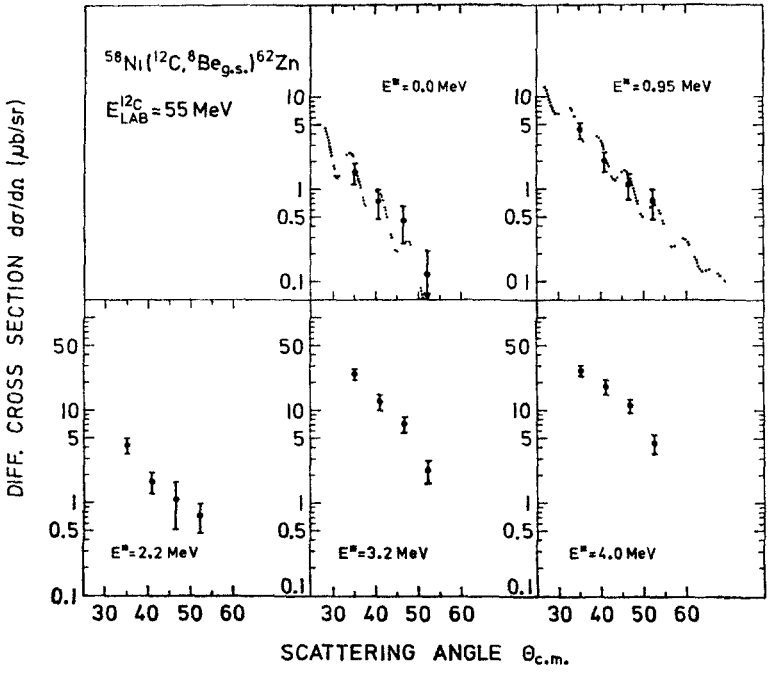

Fig. 18. Cross sections for the ^{58}Ni(^{12}C, ^{8}Be$_{g.s.}$)^{62}Zn reaction measured at an incident energy of $E_{^{12}C}$(lab) = 55 MeV for the g.s. and excited states in ^{62}Zi around 0.95, 2.2, 3.2 and 4.0 MeV. For the ground and first excited state DWBA calculations (dotted curves) are included which were obtained with the parameter values listed in tables 2 and 3, these calculations are described in subsect. 4.3.

4. Spectroscopic factors and comparison with other reactions

The angular distributions for (^{12}C, ^{8}Be) reactions on sd and fp shell nuclei are suggestive of a one-step direct transfer process, as shown in the previous section. Only the angular distribution for the ^{12}C and ^{16}O target nuclei show evidence for contributions of more complicated reaction mechanisms, such as compound and multi-step processes If, in addition to the direct character of the reaction, the transfer mechanism can be described by the transfer of an α-particle, a reasonable description of the angular distributions in terms of DWBA calculations can be made This question was investigated by using the finite range DWBA code LOLA of DeVries [15]) which treats recoil effects exactly.

For the reactions studied here (target spin = 0) the experimental cross section $d\sigma(\theta)/d\Omega$ is compared with the DWBA cross section $d\sigma(\theta)_{LOLA}/d\Omega$ by

$$\frac{d\sigma}{d\Omega}(\theta) = \frac{2J_B+1}{2J_A+1} S_\alpha(^{12}C) S_\alpha(B) \frac{d\sigma}{d\Omega}(\theta)_{LOLA}, \quad (1)$$

where A denotes the target nucleus and B the state in the residual nucleus reached in the reaction and J_A and J_B are their respective spins; $S_\alpha(^{12}C)$ is the spectroscopic factor for $^{12}C = {}^{8}Be + \alpha$ and $S_\alpha(B)$ is the respective spectroscopic factor for the residual state.

The following assumptions were made to perform the calculations: the transferred particle is an α-cluster with spin 0. Core excitations are not taken into account This means that the α-particle in the projectile $^{12}C = {}^{8}Be + \alpha$ has a relative orbital angular momentum of $l_1 = 0$. Since only spin-zero target nuclei are investigated in this paper the spin of the core A in the residual state $A + \alpha$ has spin zero and the total spin of the residual state equals the orbital angular momentum l_2. The quantity l_2 is the angular momentum transferred by the α-particles and is $l_2 = 0$, 2 or 4 for the reactions investigated here

The number of nodes N of the wave functions for the bound states of the α-particle in the final state, i.e. $\alpha + A$, is given by

$$2N + L = \sum_{i=1}^{4} 2n_i + l_i,$$

where $L = l_2$ is the angular momentum of the α-particle in the final state and n_i and l_i are the spins and orbital angular momenta of the four nucleons. To calculate the number of nodes, particular configurations of the four nucleons in the projectile and in the final state have to be made. For the projectile ^{12}C the four nucleons which form the α-particle are assumed to be in a $(1p)^4$ configuration The configurations assumed for the final states are listed in table 2

By comparing the calculated and measured cross sections the product of the spectroscopic factors $S_\alpha = S_\alpha(^{12}C)\, S_\alpha(A+\alpha)$ can be obtained. We use the index α for indicating that we are dealing with α-spectroscopic factors. In principle, for a com-

TABLE 2

Assumed shell-model configurations and bound state radius parameter r_0 ($R = r_0 A^{\frac{1}{3}}$) in the DWBA calculations for various final states and the resultant spectroscopic factors (see text)

Final state	Configuration assumed	L	N	Bound state r_0 (fm)	Binding energy (MeV)	Product $S_\alpha(^{12}C)S_\alpha(B)$	$\frac{S_\alpha(B^*)}{S_\alpha(B_{g.s.})}$	$S_\alpha(B)$
^{12}C(0$^+$, 0 0)	^{8}Be⊗(1p)^4	0	2	1.25	−7.37			0.542 [a]
^{16}O(0$^+$, 0 0)	^{12}C⊗(1p)^4	0	2	1.25	−7 16	0.125	1	0.23 [a]
^{16}O(2$^+$, 6 9)	^{12}C⊗(1p)^4	2	1	1.25	−0 26	0.45	3 6	0 83
^{20}Ne(0$^+$, 0 0)	^{16}O⊗(2s1d)^4	0	4	1 25	−4 73	0 160	1	0 295 [b]
^{20}Ne(2$^+$, 1 63)	^{16}O⊗(2s1d)^4	2	3	1.25	−3 10	0 0982	0.61	0.181
^{20}Ne(4$^+$, 4 25)	^{16}O⊗(2s1d)^4	4	2	1.25	−0 48	0 0409	0 26	0 075
^{28}Si(0$^+$, 0 0)	^{24}Mg⊗(2s1d)^4	0	4	1.25	−9 986	1 4	1	2 58
^{28}Si(2$^+$, 1 8)	^{24}Mg⊗(2s1d)^4	2	3	1.25	−8.186	0.26	0 19	0 48
^{28}Si(4$^+$, 4 6)	^{24}Mg⊗(2s1d)^4	4	2	1.25	−5.386	0.12	0 086	0 22
^{28}Si(4$^+$, 6.9)	^{24}Mg⊗(2s1d)^4	4	2	1 25	−3 086	0 39	0 29	0 72
^{30}Si(2$^+$, 5.6)	^{26}Mg⊗(2s1d)^4	2	3	1.25	−5 05	0 19		0 35
^{30}Si(2$^+$, 7.3)	^{26}Mg⊗(2s1d)^4	2	3	1.25	−3 35	0.16		0 295
^{44}Ti(0$^+$, 0 0)	^{40}Ca⊗(1f2p)^4	0	6	1.20	−5 235	0 34	1	0 62
^{44}Ti(2$^+$, 1 08)	^{40}Ca⊗(1f2p)^4	2	5	1 20	−4 155	0 0752	0.22	0 139
^{44}Ti(4$^+$, 2.5)	^{40}Ca⊗(1f2p)^4	4	4	1.20	−2.725	0.048	0.14	0.089
^{52}Ti(0$^+$, 0.0)	^{48}Ca⊗(1f2p)^4	0	6	1 20	−7.673	0.488	1	0 90
^{52}Ti(2$^+$, 1 04)	^{48}Ca⊗(1f2p)^4	2	5	1 20	−6 683	0 0328	0 067	0 061
^{52}Ti(4$^+$, 2 3)	^{48}Ca⊗(1f2p)^4	4	4	1 20	−5.373	0 0172	0 035	0 032
^{58}Ni(0$^+$, 0 0)	^{54}Fe⊗(1f2p)^4	0	6	1 25	−6 408	0.046	1	0 085
^{58}Ni(2$^+$, 1.45)	^{54}Fe⊗(1f2p)^4	2	5	1.25	−4 908	0 0080	0.17	0.015
^{58}Ni(4$^+$, 2 45)	^{54}Fe⊗(1f2p)^4	4	4	1.25	−3 908	0 0036	0 078	0 0066
^{62}Zn(0$^+$, 0 0)	^{58}Ni⊗(1f2p)^4	0	6	1.25	−3.305	0.106	1	0 20
^{62}Zn(2$^+$, 0 95)	^{58}Ni⊗(1f2p)^4	2	5	1.25	−2.355	0.038	0 35	0.070

[a]) Taken from ref. [16]).
[b]) Taken from ref [18]).

parison with other reactions the spectroscopic factor $S_\alpha(A+\alpha)$ is needed, i e., the spectroscopic factor $S_\alpha(^{12}C)$ and those for the projectiles from the other reactions to be compared with have to be known. Since these factors are not known accurately in most cases it is useful to compare the ratios of the spectroscopic factors for the excited final states and the ground state for the various reactions. In the following we will refer to this relative α-spectroscopic factor as $S_{rel} = S_\alpha(exc)/S_\alpha(g\ s)$. For the comparison of absolute spectroscopic factors we have used a value of $S_\alpha(^{12}C) = 0.542$ This value was calculated by Rotter [16]), and is close to a value of 0.675 obtained semi-empirically from the data of Gutbrod *et al.* [17]) for the ^{12}C(d, ^{6}Li)^{8}Be reaction with $S_\alpha(^{6}Li)S_\alpha(^{12}C) = 0\ 759$ and from a value of $S_\alpha(^{6}Li) = 1.1$ obtained by Klages *et al.* [17]). Theoretical values for the α-spectroscopic factor for ^{12}C and ^{16}O by Rotter [16]) were chosen for comparison with the (^{16}O, ^{12}C) reaction.

Table 3 summarizes the optical model parameters used in the DWBA calculations for the various reactions. In table 2 for every final state the assumed configuration, the transferred angular momentum, the number of nodes in the wave function, the

TABLE 3

Optical model parameters used in the DWBA calculations

Channel	V (MeV)	W_{vol} (MeV)	r_0 (fm)	a (fm)	r_I (fm)	a_I (fm)	r_c (fm)	Ref
$^{12}C+^{12}C$ $^{8}Be+^{16}O$	14	$0.4+0.14E_{c\,m}$	1.339	0.49	1.339	0.49	1 2	[23]
$^{12}C+^{16}O$ $^{8}Be+^{20}Ne$	30	12 0	1.13	0 65	1.13	0.65	1.25	[24]
$^{12}C+^{24}Mg$ $^{8}Be+^{28}Si$	37	78.0	1.28	0.583	1.305	0.28	1.25	[24]
$^{12}C+^{26}Mg$ $^{8}Be+^{30}Si$	37	78 0	1.28	0.583	1 305	0 28	1 25	[24]
$^{12}C+^{40}Ca$ $^{8}Be+^{44}Ti$	33 4	18.0 [a]	1 271	0 55	1 176	0.05	1.2	[22]
$^{12}C+^{48}Ca$ $^{8}Be+^{52}Ti$	33.4	18 0 [a]	1 271	0 55	1 176	0.05	1.2	[22]
$^{12}C+^{54}Fe$ $^{8}Be+^{58}Ni$	35 2	61 4	1.31	0.493	1.20	0 204	1 2	[25]
$^{12}C+^{58}Ni$ $^{8}Be+^{62}Zn$	35.3	19.7	1.31	0 493	1.242	0 204	1.2	[25]

$R = r_0(A_1^{\frac{1}{3}}+A_2^{\frac{1}{3}})$.

[a]) In addition to the volume absorption a surface absorption term $4W_{surf} = 18$ MeV along with a diffuseness of $a_{surf} = 0.55$ fm was used following ref. [22])

bound state radius parameter, and the binding energies as well as the extracted values for the spectroscopic product $S_\alpha(^{12}C)S_\alpha$ (residual state), the relative spectroscopic factor S_{rel} and the absolute spectroscopic factors are given. A critical discussion on the effect of using different optical model parameters and/or different bound state radii, which were found to be most sensitive in the calculations, are given at the end of subsect. 4.3.

The cross sections calculated with the DWBA code LOLA using the values of tables 2 and 3 are shown along with the experimental angular distributions in sect. 3. The results are discussed in the following.

4.1. DWBA CALCULATIONS FOR THE (^{12}C, ^{8}Be) REACTION ON ^{12}C AND ^{16}O

For the $^{12}C(^{12}C, ^{8}Be)^{16}O$ reaction at 63 MeV bombarding energy (lab) to the ground state (0^+) and to the 6.92 MeV (2^+) state, DWBA calculations were performed and are shown in fig. 3 Since this reaction was shown to contain most likely large non-direct components, no fitting of the theoretical curve to the experimental data was tried; rather the theoretical values for the spectroscopic factors for ^{12}C and ^{16}O by Rotter [16]) were used. It is gratifying to note that in fig. 3 the calculated cross

sections are of the same order of magnitude as the experimental ones; the shape of the calculated cross sections, however, deviates considerably from the experimental one.

For the 6.92 MeV (2^+) state the DWBA curve was adjusted to the data at the most forward angles, where a direct α-transfer process is expected to be strongest The absolute spectroscopic factor for this state of $S_\alpha(^{16}\mathrm{O}, 6\,9\ \mathrm{MeV}) = 0\,83$ is about four times larger than the theoretical value for the ^{16}O ground state Since the 6.92 MeV (2^+) state is the second member of the 4p-4h rotational band in ^{16}O, the obtained spectroscopic factor appears to be plausible. On the other hand the poor description of the experimental data by the theoretical curves for the ground state and the 6 92 MeV state is, in agreement with the results of subsect. 3.1 2, interpreted as evidence that significant non-direct contributions are present in this reaction.

For the ^{16}O(^{12}C, ^{8}Be)^{20}Ne reaction unsatisfactory agreement of the DWBA calculations with the experimental data is obtained (see fig. 5). Again, for the ground-state transition theoretical α-spectroscopic factors were utilized. For the 1 63 MeV (2^+) and the 4 25 MeV (4^+) states the theoretical curve was adjusted to the data at the most forward angles yielding spectroscopic factors of $S_\alpha(^{20}\mathrm{Ne}_{1\,63}) = 0\,181$ and $S_\alpha(^{20}\mathrm{Ne}_{4.25}) = 0\,075$. These values are smaller than those calculated by Matsuse and Kamimura [18]), who find a value of about 0 27 for both the 2^+ and the 4^+ states

The calculation of cross sections to unbound states in $^{20}\mathrm{Ne} = {}^{16}\mathrm{O}+\alpha$, above 4 73 MeV excitation energy, are not possible with the computer code used.

4 2. DWBA CALCULATIONS FOR THE (^{12}C, ^{8}Be) REACTION ON sd SHELL NUCLEI

The experimental angular distributions for the ^{24}Mg and ^{26}Mg targets (see subsect 3.2) clearly show a direct reaction character. Therefore a better description of the data in terms of DWBA calculations is expected than for the light target nuclei described in the previous section.

In fig. 8, DWBA predictions for the reaction ^{24}Mg(^{12}C, ^{8}Be)^{28}Si at 65 MeV bombarding energy are compared with the experimental data between 20° and 80° (c m.). As can be seen, the calculations are in reasonable agreement with the data; in particular, the rapid decrease of the cross section with angle over three orders of magnitude is correctly reproduced by the calculations A spin of 4^+ has been assumed for the calculation corresponding to the 6.9 MeV state, i.e., it is assumed that the 6.89 (4^+) state is much more strongly excited than the 6.88 (3^-) state. This is suggested from the work of Lindgren *et al* [19]). Since the calculations are lengthy and expensive the possible influence of the 3^- state has not been investigated here.

The absolute α-spectroscopic factors obtained for the states in ^{28}Si are relatively large: a value of 2 58 is found for the ground state, and decreases with increasing spin of the final state to 0.48 for the 2^+ state and to 0 22 for the 4^+ state at 4 6 MeV As expected, the 6 9 MeV state has a large spectroscopic factor of 0.72. These spectroscopic factors are close to those for ^{12}C, ^{16}O and ^{20}Ne and suggest that similar α-structures exist in ^{28}Si.

Using the same parameters and spectroscopic factors as before, DWBA predictions

were made for the angular distributions between $-2°$ and 40° (c.m.) measured at 50 MeV and shown in fig. 7. Whereas the ground-state angular distribution is described adequately at the most forward angles, the data for the other states are significantly larger at angles between 0° and 10° than the DWBA cross sections. For angles larger than about 10° satisfactory agreement, comparable to the 65 MeV data in fig. 8, is obtained here also. This effect is interesting and has been observed also for one-proton transfer reactions by Sink *et al* [20]). These authors attribute the enhanced cross section at small angles to interference effects For a discussion of interference effects at small angles we would like to refer also to the work of Ascuitto and Glendenning [21])

The DWBA curves in fig. 10 for the ^{26}Mg(^{12}C, ^{8}Be)^{30}Si reaction are in agreement with the data within the large experimental error bars Therefore the extracted spectroscopic factors are associated with uncertainties of up to 50 %. However, they are smaller than the corresponding ones to ^{28}Si (see table 2).

In summary of the DWBA calculations for the sd shell nuclei, it can be concluded that the experimental data are consistent with the assumption of an α-transfer mechanisms for the (^{12}C, ^{8}Be) reaction Only at very forward angles, where data were taken for the ^{24}Mg(^{12}C, ^{8}Be)^{28}Si reaction, are the experimental cross sections found to be considerably larger than the calculated ones.

4.3. DWBA CALCULATIONS FOR THE (^{12}C, ^{8}Be) REACTION ON fp SHELL NUCLEI

DWBA cross sections have been calculated for the (^{12}C, ^{8}Be) reaction on the target nuclei ^{40}Ca, ^{48}Ca, ^{54}Fe and ^{58}Ni utilizing the optical model potentials listed in table 3 and the spectroscopic assumptions in table 2.

In fig 12, calculated cross sections for the ^{40}Ca(^{12}C, ^{8}Be)^{44}Ti reaction at 56 MeV bombarding energy are compared with the experimental data for the ground state (0^+) and for the 1.08 MeV (2^+) and the 2.5 MeV (4^+) final states. The optical potential of Bond *et al.* [22]) obtained for ^{13}C + ^{40}Ca elastic scattering was used. Whereas good agreement with the data is achieved for the 2^+ and 4^+ states the strong oscillations in the theoretical ground-state angular distribution is not observed in the data. A possible reason is that the experimental data were taken with an angular resolution of $\pm 2°$, in order to achieve large detection efficiencies for ^{8}Be. The overall decrease of the experimental and theoretical cross sections for the ground-state transition are in agreement. Absolute α-spectroscopic factors of 0.62, 0.139 and 0 089 are obtained for the ground state, 2^+ and 4^+ states, respectively, showing a decrease with increasing spin of the final state. This behavior was also observed for the sd shell nuclei (see subsect 4.2).

The results for the ^{48}Ca(^{12}C, ^{8}Be)^{52}Ti reactions are shown in fig. 14. Because of the lack of optical model parameters from ^{12}C + ^{48}Ca elastic scattering, the same potential as before is used here (see table 3). Similar to the ^{40}Ca reaction the ground-state angular distribution oscillates strongly with angle. The relatively smooth decrease of the experimental cross sections, again, is most likely due to the angular spread-

ing of $\pm 2°$ in data taking. For the 2^+ and 4^+ states the experimental cross sections seem to fall off more rapidly for angles larger than 40° than predicted by the calculations. The resultant α-spectroscopic factors for the 2^+ and 4^+ states in ^{52}Ti are about two to three times smaller than the corresponding ones in ^{44}Ti. A comparison of the ground-state spectroscopic factors is hardly meaningful because of the large uncertainties in determining these values for both the ^{44}Ti and the ^{52}Ti ground states.

For the ^{54}Fe(^{12}C, ^{8}Be)^{58}Ni and the ^{58}Ni(^{12}C, ^{8}Be)^{62}Zn reactions, DWBA calculations are shown in figs 16 and 18, respectively. As can be seen in table 2, the α-spectroscopic factors for states in ^{58}Ni are extremely small, they are even smaller than those for ^{52}Ti. This is not expected if four-nucleon correlations are assumed for these states (see sect. 3). For ^{62}Zn the α-spectroscopic factors are larger again, i.e., they are 0.20 for the ground state and 0.07 for the 2^+ state. It is interesting to note that the oscillations in the calculated ground-state angular distribution are less pronounced than for the other fp shell nuclei studied in this paper.

The DWBA cross sections depend strongly on the bound state radius parameter (here: for $\alpha + {}^{8}$Be) and to a certain degree on the choice of the optical model parameters. Whereas an order of magnitude difference was found for the spectroscopic factors for the ^{40}Ca(^{12}C, ^{8}Be)^{44}Ti reaction for bound state radii for $\alpha + {}^{8}$Be of $R = 1\,2\,A_{^{8}\mathrm{Be}}^{\frac{1}{3}} = 2.4$ fm and $R = 1.2\,(A_{^{8}\mathrm{Be}}^{\frac{1}{3}} + A_{\alpha}^{\frac{1}{3}}) = 4.3$ fm, the difference from different optical model parameters was found to be less than 25 %. The absolute α-spectroscopic factors therefore are strongly model-dependent; for the relative spectroscopic factors, however, no significant change was observed from different ground-state radii or optical model parameters

TABLE 4

Comparison of relative spectroscopic factors $S_{\mathrm{rel}} = S_{\alpha}(E_x)/S_{\alpha}(\mathrm{g.s.})$ as extracted from (^{6}Li, d), (^{12}C, ^{8}Be) and (^{16}O, ^{12}C) reactions (see text)

Final state	(^{6}Li, d)	Ref.	(^{12}C, ^{8}Be) present work	(^{16}O, ^{12}C)	Ref.
^{16}O(6.9 MeV, 2^+)	2 3 [a])	[26])	3.6		
^{23}Ne(1 63, 2^+)	0 26	[27])	0.61		
^{20}Ne(4 25, 4^+)	0.19	[27])	0.26		
^{28}Si(1.8, 2^+)	0.21	[28])	0.19	0.22 0.27	[29]) [20])
^{28}Si(4.6, 4^+)	0.10	[28])	0.09		
^{44}Ti(1.08, 2^+)	0.26	[30])	0.22	0.49	[31])
^{44}Ti(2.5, 4^+)	0.15	[30])	0.14		
^{44}Ti(3.34, 4^+)				0.14	[31])
^{52}Ti(1.04, 2^+)	0.46	[32])	0.067		
^{58}Ni(1.45, 2^+)	0.28	[32])	0.17		
^{62}Zn(0 95, 2^+)	0.23	[32])	0.35		

[a]) This value was extracted from the (^{7}Li, t) reaction.

4 4 COMPARISON OF SPECTROSCOPIC FACTORS FROM DIFFERENT FOUR-NUCLEON TRANSFER REACTIONS

In table 4, α-spectroscopic factors from the (^{12}C, ^{8}Be) reaction obtained in this work are compared with those from other four-nucleon transfer reactions where available

4 4.1 Light target nuclei. Considering the large uncertainties in the reaction mechanism, a surprisingly good agreement of the spectroscopic factors for the (^{6}Li, d), (^{7}Li, t) and (^{12}C, ^{8}Be) reaction is obtained for light target nuclei in table 4 It is also interesting to note that the spectroscopic factor for the 6.9 MeV (2^+) state in ^{16}O is about a factor of three times larger than the ground-state one For the ^{20}Ne g.s. band, decreasing spectroscopic factors are obtained with increasing spin This is not in agreement with theoretical estimates and a possible reason could be that compound contributions are larger for the reactions which lead to final states with relatively large spins

4 4.2. The sd shell nuclei Relative spectroscopic factors for states in ^{28}Si, extracted from the (^{6}Li, d), (^{12}C, ^{8}Be) and (^{16}O, ^{12}C) reactions are compared in table 4. A strikingly good agreement is obtained, suggesting a simple α-transfer process for these reactions.

4.4 3. The fp shell nuclei. Excellent agreement of the spectroscopic factors for the ground-state band in ^{44}Ti is obtained from the (^{6}Li, d) and (^{12}C, ^{8}Be) reaction (see table 4), whereas the agreement with (^{16}O, ^{12}C) is poorer. For ^{52}Ti the extracted values deviate considerably. A somewhat better agreement is observed for ^{58}Ni and ^{62}Zn, as can be seen in table 4.

5. Conclusion

From the spectra, angular distributions and DWBA calculations presented in this paper it is concluded that the (^{12}C, ^{8}Be) reaction from the target nuclei ^{12}C, ^{16}O, ^{24}Mg, ^{26}Mg, ^{40}Ca, ^{48}Ca, ^{54}Fe and ^{58}Ni investigated in this paper exhibit both direct and non-direct features for the light target nuclei ^{12}C and ^{16}O and show a clearly dominant direct reaction mechanisms for target nuclei of ^{24}Mg and heavier. Indications are: The particle spectra for the (^{12}C, ^{8}Be) reactions on ^{12}C and ^{16}O show strong excitations of "α-like" states; however, other non "α-like" states are also excited including states with unnatural parity. A 10–30 % compound contribution, found in the analysis of the excitation functions [9]), is consistent with the results obtained here The poor agreement of the DWBA calculation with the shape of the experimental angular distributions is likely to be due to the compound contribution in the reaction On the other hand, the agreement of the spectroscopic factors with other four-nucleon transfer reactions such as (^{6}Li, d), is indicative that the reaction to the strongly excited α-like states is mainly direct. This is also confirmed from the spectra at very forward angles, where a strong population of the α-like states are observed

The (^{12}C, ^{8}Be) reaction from the target nuclei of ^{24}Mg and heavier clearly indicate a direct reaction mechanism: the cross section decreases rapidly with angle and good agreement with the DWBA calculations is obtained. No indication is found for the population of unnatural parity states in any of the spectra.

Some support for the assumption of an α-transfer mechanism in contrast to a more complicated transfer of four nucleons is obtained from the good agreement of the spectroscopic factors with other reactions such as (^{6}Li, d) and (^{16}O, ^{12}C), and the selective excitation of the same final states in all of these reactions.

We would like to thank Dr. Kemmer and Frau Weismann for the fabrication of the solid-state detectors and Dr. Maier and Frl. Frischke for the preparation of the targets. Discussions with Dr. DeVries and his help concerning the LOLA computer code are gratefully acknowledged. We would also like to thank Dr. Münzer and Dr. Rohrer as well as the tandem operators for making an intense carbon beam available from the Munich MP tandem.

References

1) K. Bethge, Ann. Rev Nucl. Sci. **20** (1970) 255
2) H. Faraggi, A. Jaffrin, M. C. Lemaire, M C Mermaz, J. C. Faivre, J. Gastebois, B. G. Harvey, J.-M. Loiseaux and A. Papineau, Ann. of Phys. **66** (1971) 905,
H. Faraggi, M.-C. Lemaire, J -M. Loiseaux, M. C. Mermaz and A. Papineau, Phys. Rev. **C4** (1971) 1375
3) R. M. DeVries, Nucl. Phys. **A212** (1973) 207, and Phys. Rev. **C8** (1973) 951
4) U. Strohbusch, C. L. Fink, B. Zeidman, R. G. Markham, H W Fulbright and R. N. Horoshko, Phys. Rev **C9** (1974) 965
5) D. Robson, Comments Nucl. Particle Phys. **5** (1972) 16
6) J. G Cramer, K. A. Eberhard, N R. Fletcher, E. Mathiak, H. H. Rossner and A. Weidinger, Nucl. Instr. **111** (1973) 425
7) L. C. Northcliffe and R. F. Schilling, Nucl. Data Tables **7** (1970) 234
8) J Stettmeier, Diploma Thesis, Universitat Munchen, 1974 (unpublished)
9) A. Weidinger, K. A Eberhard, E. Mathiak, J Stettmeier, W. Trombik and L. N Wustefeld, Nucl. Phys **A257** (1976) 144
10) K A. Eberhard, E. Mathiak, J. Stettmeier, A Weidinger, L. N. Wustefeld and K. G. Bernhardt, Phys Lett. **56B** (1975) 445
11) K A. Eberhard and K G. Bernhardt, Phys. Rev. **C13** (1976) 440
12) F D Becchetti, in Proc. of heavy ion summer study, Oak Ridge National Laboratory, June 12–July 1, 1972 Conf. 720669, p. 163
13) H. Kusakari, T Suehiro, M Ishihara, H. Kawakami, N. Joschikawa and M. Sakai, J Phys. Soc Jap **34** (1973) 865
14) L. C. Farwell, J. J. Kraushaar and H. W. Bear, Bull Am. Phys. Soc. **16** (1971) 626, and Nucl. Phys. **A186** (1972) 545
15) R. M. DeVries, Computer Code LOLA, 1973
16) I. Rotter, Fortschritte der Physik **16** (1968) 195
17) H. H Gutbrod, H. Yoshida and R. Bock, Nucl. Phys. **A165** (1971) 240,
W. J. Klages, H. H Duhm, H. Yoshida, P E Schumacher and C. Detraz, Nucl. Phys. **A156** (1970) 65
18) T. Matsuse and M Kamimura, Prog. Theor. Phys. **49** (1973) 1765
19) R. A. Lindgren, J P. Trentelman, N. Anantaraman, H. E. Gove and F. C. Jundt, Phys. Lett. **49B** (1974) 263

20) D A Sink, C M Cheng, J. C. Peng and H S. Song, Report of Curr Research, 1973/74, University of Pittsburgh, p 20
21) R. I. Ascuitto and N K. Glendenning, Phys. Lett. **48B** (1974) 6
22) P D Bond, J. D Garrett, S. Kahana, M J LeVine and A Z Schwarzschild, in Reactions between complex nuclei, ed. R L. Robinson, F. K McGowan, J B. Ball and J. H Hamilton (North-Holland, Amsterdam, 1974) p 54
23) W. Reilly, R. Wieland, A. Gobbi, M. W. Sachs, J. V. Maher, D Mingay, R. H. Siemssen and D. A. Bromley, in Nuclear reactions induced by heavy ions, ed R Bock and W. Hering (North-Holland, Amsterdam, 1970) p 95
24) R M. DeVries, private communication, 1975
25) M.-C Lemaire, M. C Mermaz, H Sztark and A. Cunsolo, in Reactions between complex nuclei, ed. R L. Robinson, F. K McGowan, J. B. Ball and J. H Hamilton (North-Holland, Amsterdam) p. 21
26) F Puhlhofer, H. G. Ritter and R Bock, Nucl Phys **A147** (1970) 258
27) N. Anantaraman, R. M DeVries, I. P Draayer, H. E. Gove and J. P. Trentelman, in Reactions between complex nuclei, ed. R L Robinson, F. K. McGowan, J. B Ball and J. H. Hamilton (North-Holland, Amsterdam, 1974) p. 43
28) I. P Draayer, H E. Gove, J P. Trentelman, N Anantaraman and R M. DeVries, Phys. Lett. **53B** (1974) 250
29) J R Erskine, W Henning, D. G. Kovar, L R. Greenwood and R. M. DeVries, Phys Rev. Lett. **34** (1975) 680
30) U. Strohbusch, G Bauer and H. W Fulbright, Phys Rev Lett **34** (1975) 968
31) R. M DeVries, Phys Rev Lett. **30** (1973) 666
32) G Bauer and U Strohbusch, private communication